The Astrophysical Journal, 646:474–479, 2006 July 20
© 2006. The American Astronomical Society. All rights reserved. Printed in U.S.A.

DEBRIS DISKS AROUND WHITE DWARFS: THE DAZ CONNECTION

Mukremin Kilic,[1,2] Ted von Hippel,[2] S. K. Leggett,[1,3] and D. E. Winget[2]

Received 2006 January 18; accepted 2006 March 27

ABSTRACT

We present near-infrared spectroscopic observations of 20 previously known DAZ white dwarfs obtained at the NASA Infrared Telescope Facility. Two of these white dwarfs (G29-38 and GD 362) are known to display significant *K*-band excesses due to circumstellar debris disks. Here we report the discovery of excess *K*-band radiation from another DAZ white dwarf, WD 0408−041 (GD 56). Using spectroscopic observations, we show that the excess radiation cannot be explained by a stellar or substellar companion, and is likely to be caused by a warm debris disk. Our observations strengthen the connection between the debris disk phenomena and the observed metal abundances in cool DAZ white dwarfs. However, we do not find any excess infrared emission from the most metal rich DAZs with $T_{\rm eff} = 16,000$–$20,000$ K. This suggests that the metal abundances in warmer DAZ white dwarfs may require another explanation.

Subject heading: stars: individual (WD 0408−041, GD 56) — white dwarfs

Online material: color figures

1. INTRODUCTION

The presence of planets around solar-type stars suggests that some white dwarfs should have planetary systems as well. Even though planets within 5 AU of their parent stars will most likely not survive the red giant phases, most of the outer planets, Kuiper belt objects, and Oort-like comet clouds are predicted to survive around white dwarf stars (Debes & Sigurdsson 2002; Burleigh et al. 2002). Near- and mid-infrared searches for stellar and substellar companions to white dwarfs have resulted in the discovery of late-type dwarfs and two brown dwarfs (Farihi et al. 2005), but no planetary systems yet (F. Mullally et al. 2006, in preparation). The search for the effects of reflex orbital motion in changing light travel times caused by possible planetary companions to pulsating white dwarfs (Winget et al. 2003) has provided strong limits on one object so far, G117-B15A (Kepler et al. 2005). Finding a Jupiter-size planet around an intrinsically faint Earth-size white dwarf would herald a new age of direct studies of extrasolar planets.

An easier way to detect the signatures of planetary systems around white dwarfs is via debris disks. Previously stable orbits of planets around a star undergoing mass loss may become unstable, which in some systems may result in close encounters leading to tidal stripping of a parent body, thus producing a circumstellar debris disk (Debes & Sigurdsson 2002; Jura 2003). Until recently, there was only a single white dwarf known to have a circumstellar debris disk, G29-38 (see Chary et al. 1999). G29-38 is a pulsating DAZ white dwarf with a hydrogen-rich atmosphere that has trace amounts of metals. Infrared excess around this white dwarf was initially thought to be due to a brown dwarf companion (Zuckerman & Becklin 1987); however, follow-up observations in the near- and mid-infrared showed that the excess emission is caused by a debris disk. Reach et al. (2005) discovered silicate emission around G29-38 and could explain the observed mid-infrared spectrum by a combination of amorphous olivine, amorphous carbon, and crystalline forsterite. These observations suggest a relatively recent disruption of one or perhaps a few comets or asteroids around this white dwarf.

The presence of metals in the photosphere of G29-38 is probably related to the presence of a dust disk around the star. Possible scenarios for the explanation of the metal abundances in DAZ white dwarfs include accretion from the interstellar medium (ISM; Dupuis et al. 1992), cometary impacts (Alcock et al. 1986), and accretion of asteroidal material from a surrounding debris disk (Graham et al. 1990). If accretion from the ISM is responsible for the observed metal abundances, we would expect to find cool DAZs only near interstellar clouds, since the diffusion timescales for the metals in their photospheres (∼years) are shorter than the cloud crossing timescales ($\geq 10^4$ yr). Yet Zuckerman et al. (2003) did not find any correlation between the locations and relatively large numbers of DAZs and the locations and amount of ISM present within the local bubble.

The discovery of the most massive (1.24 $M_\odot$) and metal-rich white dwarf currently known, GD 362, by Gianninas et al. (2004) and Kawka & Vennes (2005, 2006) stimulated a search for a debris disk around it. GD 362 is the most extreme DAZ star, with nearly solar iron and magnesium abundances [$\log({\rm Fe/H}) = -4.5$ and $\log({\rm Mg/H}) = -4.8$]. A breakthrough came 18 years after the discovery of a debris disk around G29-38 when Becklin et al. (2005) and Kilic et al. (2005) discovered significant excess infrared radiation from GD 362. The observed near- and mid-infrared excess around this star could only be explained by a circumstellar debris disk. These recent results support the idea that accretion from a surrounding debris disk can explain the metal abundances observed in cool DAZ white dwarfs.

Calcium abundances[4] for known DAZs (Zuckerman et al. 2003; Gianninas et al. 2004; Berger et al. 2005) range from $[{\rm Ca/H}] = -5.2$ to -12.7. Several stars are more metal-rich than G29-38 ($[{\rm Ca/H}] = -6.9$), providing a unique opportunity to test whether the observed metal abundances can be explained with

[1] Visiting Astronomer at the Infrared Telescope Facility, which is operated by the University of Hawaii under Cooperative Agreement NCC 5-538 with the National Aeronautics and Space Administration, Office of Space Science, Planetary Astronomy Program.

[2] Department of Astronomy, University of Texas at Austin, 1 University Station C1400, Austin, TX 78712; kilic@astro.as.utexas.edu.

[3] Joint Astronomy Centre, 660 North A'ohoku Place, University Park, Hilo, HI 96720.

[4] [Ca/H] is the logarithm of the Ca/H abundance ratio by number.

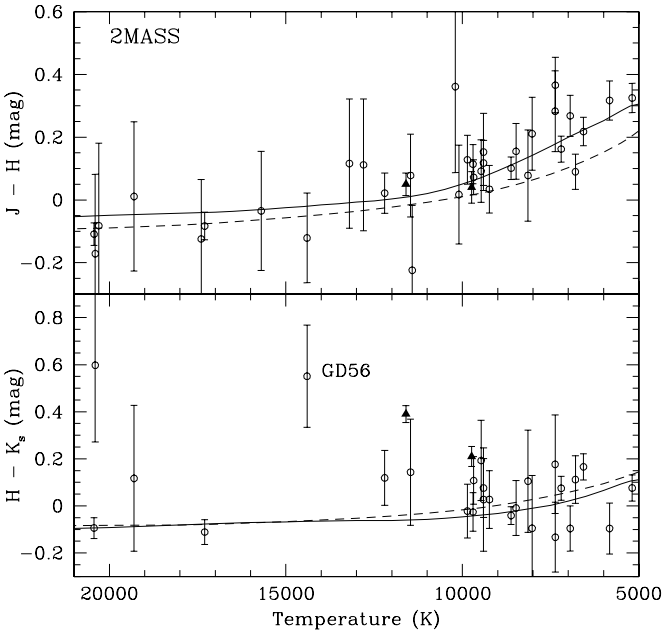


FIG. 1.—$J - H$ and $H - K$ 2MASS colors vs. temperature for single DAZ white dwarfs (*open circles*) studied by Berger et al. (2005). The predicted sequences for DA (*solid line*) and DB (*dashed line*) white dwarfs and the colors for G29-38 and GD 362 (*filled triangles*) are also shown. GD 56, a likely debris disk candidate from 2MASS photometry, is labeled.

debris disks similar to G29-38 and GD 362. With a goal of determining the fraction of DAZs with detectable near-infrared excess emission from warm debris disks, we obtained near-infrared spectroscopy of 20 DAZ white dwarfs, including G29-38 and GD 362. Our observations are discussed in § 2, while an analysis of the spectroscopic data and results from this analysis are discussed in § 3.

2. OBSERVATIONS

2.1. *Photometry*

All of the DAZ white dwarfs identified by Zuckerman et al. (2003) and Koester et al. (2005) are bright enough to be detected in the Two Micron All Sky Survey (2MASS). However, the 2MASS photometry in the H and K bands is inaccurate for the majority of the objects, making the search for infrared excess around these objects unreliable. Figure 1 presents 2MASS photometry versus effective temperatures for single DAZ white dwarfs studied by Berger et al. (2005), along with the predicted sequences for DA (*solid line*) and DB white dwarfs (*dashed line*) from Bergeron et al. (1995). The 2MASS photometry for G29-38 and the 3 m NASA Infrared Telescope Facility (IRTF) photometry for GD 362 (*filled triangles*) are also plotted. Several objects are only detected in the J and H bands, but not in the K band, and are therefore not included in the bottom panel. Even though the large error bars in 2MASS photometry prevent any definitive conclusion, it is clear from this figure that several objects, most notably GD 56, show excess K-band flux at the 2–3 σ level.

2.2. *Spectroscopy*

We used the 0.8–5.4 Micron Medium-Resolution Spectrograph and Imager (SpeX; Rayner et al. 2003) on IRTF and a 0.″5 slit to obtain a resolving power of 90–210 (average resolution of 150) over the 0.8–2.5 μm range. Our observations were performed under conditions of thin cirrus and partly cloudy skies between 2005 November 2–7. To remove the dark current and the sky signal from the data, the observations were taken in two different positions on the slit (A and B) separated by 10″. The total exposure times for individual objects ranged from 16 to 96 minutes. Internal calibration lamps (a 0.1 W incandescent lamp and an Argon lamp) were used for flat-fielding and wavelength calibration, respectively. In order to correct for telluric features and flux calibrate the spectra, nearby bright A0 V stars were observed at an air mass similar to the target star observations. We used an IDL-based package, Spextool version 3.2 (Cushing et al. 2004), to reduce our data (see Kilic et al. 2005 for details). Using the nearby A0 V star observations and the XTELLCOR package (Vacca et al. 2003), we created a telluric spectrum for each A0 V star observation, and used these spectra to flux calibrate and correct the telluric features in the white dwarf spectra.

3. RESULTS

Figure 2 presents the flux-calibrated spectra of our DAZ sample (*jagged solid lines*; ordered in $T_{\rm eff}$) and their respective DA white dwarf model atmospheres (*smooth solid lines*; kindly made available to us by D. Koester and D. Saumon). The resolutions of the model white dwarf spectra were not matched to the instrumental resolution, in order to show the predicted locations of the Paschen lines (0.955, 1.005, 1.094, 1.282, and 1.876 μm). Changing the resolutions of these models would only make the hydrogen lines shallower but not change the overall shape of the expected continuum. The observed white dwarf spectra are affected by strong telluric features between 1.35–1.45 μm, 1.80–2.05 μm, and longward of 2.5 μm (a typical telluric spectrum observed at the IRTF is presented in Fig. 3 of Kilic et al. 2005). Therefore, weak features observed in several stars in these wavelength ranges are likely to be due to telluric correction problems.

We derived synthetic colors of all 20 objects in our sample using our infrared spectra. Since our observations were performed under nonphotometric conditions, the absolute flux level in these spectra cannot be trusted. Nevertheless, the relative flux level of the spectra $J - H$ and $H - K$ colors should not be affected by the nonphotometric conditions. The photometric error bars were calculated from the observed scatter of the spectra in individual frames. Effective temperatures, gravities, calcium abundances, 2MASS photometry, and our synthetic colors for these objects are presented in Table 1. A comparison of the 2MASS colors with our synthetic colors shows that they are consistent within the errors. Figure 3 presents synthetic colors versus temperatures, and $J - H$ versus $H - K$ color for our sample. The predicted sequences for DA (*solid line*) and DB white dwarfs (*dashed line*) from Bergeron et al. (1995) are also shown. Our IRTF observations improved the photometry for these objects significantly, enabling us to use the spectroscopy and photometry to identify near-infrared excess.

A comparison of the spectroscopy and photometry for the DAZ white dwarfs in our sample shows that the majority of the stars do not show any excess emission in the near-infrared. However, the two previously known debris disk white dwarfs (G29-38 and GD 362) plus WD 0408−041 (hereafter called GD 56) show significant excess in the K band. The observed spectrum of GD 56 is consistent with a typical 14,000 K white dwarf in the J band, but it starts to deviate from a DA white dwarf model in the H band, and shows more infrared excess than either of the previously known debris disk white dwarfs. GD 56, G29-38, and GD 362 are easily distinguishable from the rest of the DAZs in our sample in Figure 3.

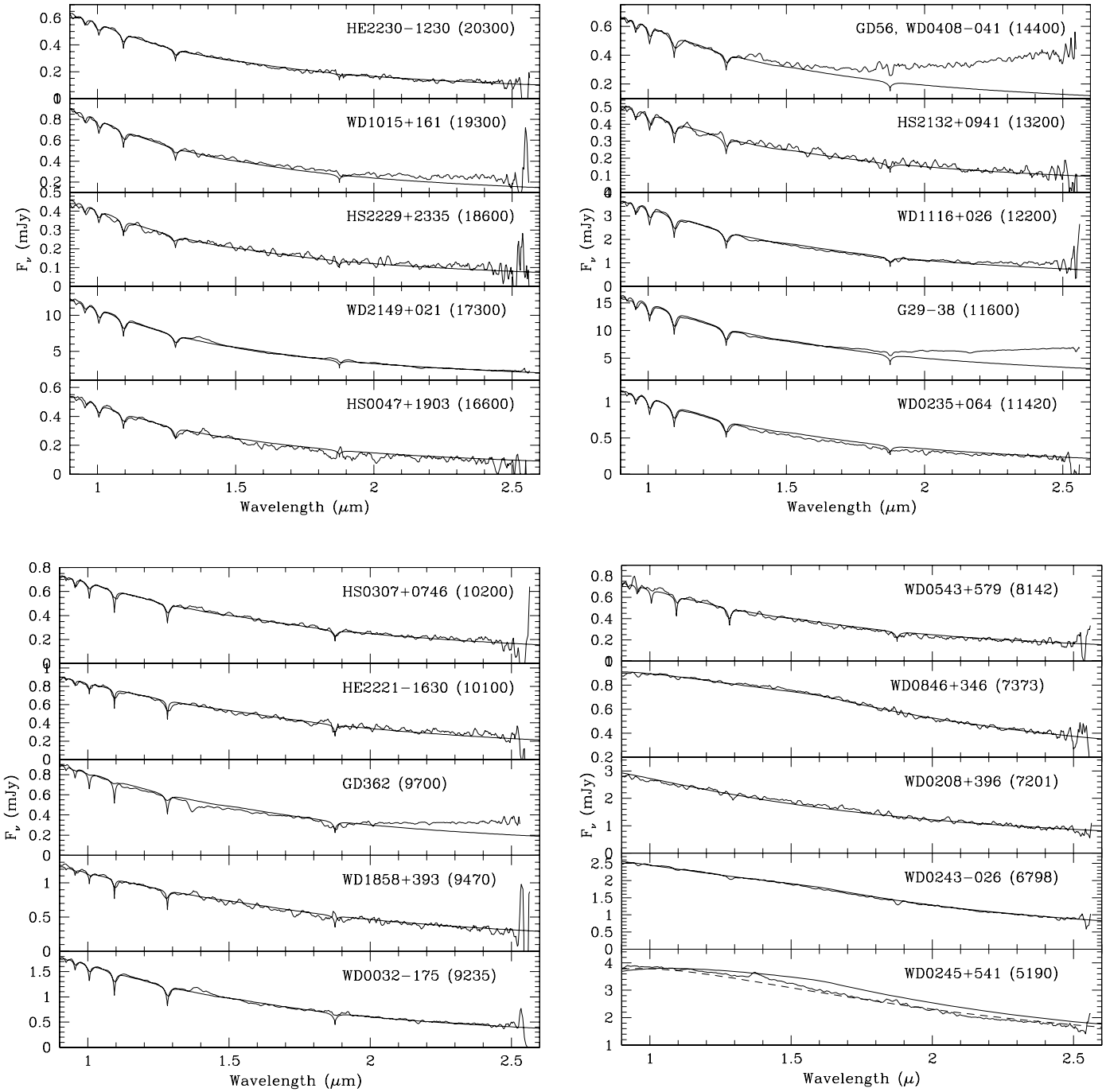


FIG. 2.—Flux-calibrated spectra of the DAZ white dwarfs in our sample (*jagged solid lines*; ordered in $T_{\rm eff}$) compared to models (*smooth solid lines*). [*See the electronic edition of the Journal for a color version of this figure.*]

There are two other objects with possible slight infrared excesses, WD 1015+161 and WD 1116+026. WD 1015+161 observations may have been affected by a nearby object, which is located 2.″1 away and is ∼0.2 mag fainter than the white dwarf at *J*. We obtained a noisy spectrum of this object that did not reveal any spectral features. The overall flux distribution of this nearby object could be approximated by an ∼8000 K blackbody. Hence the observed slight excess for WD 1015+161 ($T_{\rm eff} = 19,300$ K) in the *K* band may be caused by this nearby object. WD 1116+026 may show slight excess in the *K* band as well, although our synthetic photometry shows that the excess in $H - K$ color is less than 2 σ. This white dwarf appeared to be a single star in our guider and spectral images. Therefore, WD 1116+026 ([Ca/H] = −7.3) may be another warm debris disk case, but the observed excess and errors are consistent with photospheric flux from the white dwarf.

We note that the observed spectrum of WD 0245+541 is better fitted with a 5190 K helium-rich white dwarf model atmosphere (Fig. 2, *last panel, dashed line*) rather than a DA model atmosphere (*last panel, smooth solid line*). Only weak Hα is seen in the spectrum of cool DAs with $T_{\rm eff} \sim 5000$ K, and infrared photometry is often necessary to determine the atmospheric composition of cool white dwarfs (see Bergeron et al. 2001 for a detailed discussion). Greenstein & Liebert (1990) obtained an Hα equivalent width measurement of 0.3 Å for WD 0245+541. Their classification of this star as a DA white dwarf relies only on optical

TABLE 1
NEAR-INFRARED PHOTOMETRY OF COOL DAZs

Object	$T_{\rm eff}$ (K)	log g	[Ca/H]	$J_{\rm 2MASS}$ (mag)	$(J-H)_{\rm 2MASS}$ (mag)	$(H-K)_{\rm 2MASS}$ (mag)	$(J-H)_{\rm IRTF}$ (mag)	$(H-K)_{\rm IRTF}$ (mag)
WD 0032−175	9235	8.0	−10.2	14.79 ± 0.04	0.03 ± 0.08	0.03 ± 0.12	0.04 ± 0.04	−0.02 ± 0.04
HS 0047+1903	16600	7.8	−6.1	16.33 ± 0.11	...	...	−0.10 ± 0.09	−0.10 ± 0.15
WD 0208+396	7201	7.9	−8.8	13.83 ± 0.02	0.16 ± 0.04	0.08 ± 0.05	0.17 ± 0.03	0.01 ± 0.03
WD 0235+064	11420	7.9	−9.0	15.69 ± 0.07	−0.22 ± 0.21	...	−0.05 ± 0.04	−0.04 ± 0.08
WD 0243−026	6798	8.2	−9.9	14.68 ± 0.04	0.09 ± 0.06	0.11 ± 0.10	0.21 ± 0.03	0.01 ± 0.04
WD 0245+541	5190	8.2	−12.7	13.87 ± 0.02	0.33 ± 0.05	0.08 ± 0.06	0.25 ± 0.03	0.07 ± 0.04
HS 0307+0746	10200	8.1	−7.6	16.39 ± 0.14	0.36 ± 0.27	...	0.08 ± 0.02	−0.02 ± 0.02
WD 0408−041	14400	7.8	−7.1	15.87 ± 0.06	−0.12 ± 0.14	0.55 ± 0.22	0.16 ± 0.04	0.56 ± 0.04
G29-38	11600	8.1	−6.9	13.13 ± 0.03	0.06 ± 0.04	0.39 ± 0.04	...	...
GD 362	9740	9.1	−5.2	16.16 ± 0.09	...	...	0.04 ± 0.05	0.21 ± 0.04
WD 0543+579	8142	8.0	−10.3	15.52 ± 0.07	0.08 ± 0.15	0.11 ± 0.22	0.02 ± 0.08	−0.05 ± 0.12
WD 0846+346	7373	8.0	−9.4	15.89 ± 0.07	0.28 ± 0.13	0.18 ± 0.21	0.31 ± 0.04	0.03 ± 0.04
WD 1015+161	19300	7.9	−6.3	16.13 ± 0.09	0.01 ± 0.24	0.12 ± 0.31	0.02 ± 0.03	0.08 ± 0.03
WD 1116+026	12200	7.9	−7.3	14.75 ± 0.04	0.02 ± 0.06	0.12 ± 0.12	−0.02 ± 0.05	0.06 ± 0.07
WD 1858+393	9470	8.0	−7.8	15.53 ± 0.05	0.09 ± 0.10	0.19 ± 0.17	0.09 ± 0.03	−0.03 ± 0.05
HS 2132+0941	13200	7.7	−7.7	16.09 ± 0.08	0.12 ± 0.21	...	0.05 ± 0.06	−0.05 ± 0.09
WD 2149+021	17300	7.9	−7.6	13.20 ± 0.02	−0.08 ± 0.04	−0.11 ± 0.05	−0.05 ± 0.03	−0.06 ± 0.03
HE 2221−1630	10100	8.2	−7.6	15.80 ± 0.06	0.02 ± 0.16	−0.06 ± 0.14	0.10 ± 0.05	0.07 ± 0.04
HS 2229+2335	18600	7.9	−6.3	16.16 ± 0.09	...	...	0.02 ± 0.07	0.00 ± 0.08
HE 2230−1230	20300	7.7	−6.3	16.36 ± 0.11	−0.08 ± 0.26	...	−0.09 ± 0.08	−0.07 ± 0.12

NOTE.—Values of $T_{\rm eff}$, log g, and [Ca/H] are from Berger et al. (2005) and Gianninas et al. (2004).

spectroscopy. Our near-infrared spectrum of this object favors a helium-rich atmosphere model; therefore WD 0245+541 is more likely to be a DZA than a DAZ.

4. DISCUSSION

Figure 4 shows the IRTF spectra of GD 56, G29-38, and GD 362, along with the expected near-infrared fluxes for each star (*dashed lines*). The observed excess in GD 56 is very similar to the excess seen in G29-38 and GD 362. The expected flux levels from a 14,400 K blackbody (normalized to the observed GD 56 spectrum in the J band) in the H and K_S bands are 0.27 and 0.17 mJy, respectively. The difference between the observed and expected flux from the star is about 0.05 mJy in the H band, and 0.18 mJy in the K band. Using log $g = 7.8$ and $T_{\rm eff} = 14,400$ K (Berger et al. 2005) and Bergeron et al. (1995) models, we estimate the absolute K-band magnitude of GD 56 to be 11.43 mag. If the observed near-infrared excess is due to a late type dwarf companion, this would correspond to $M_K \sim 11.38$ mag, an early L dwarf (Leggett et al. 2002). We used an L3 dwarf template from the IRTF Spectral Library (Cushing et al. 2005) plus the normalized 14,400 K blackbody to attempt to match the observed excess in the K band (Fig. 4, *top, dotted line*). Adding an L3

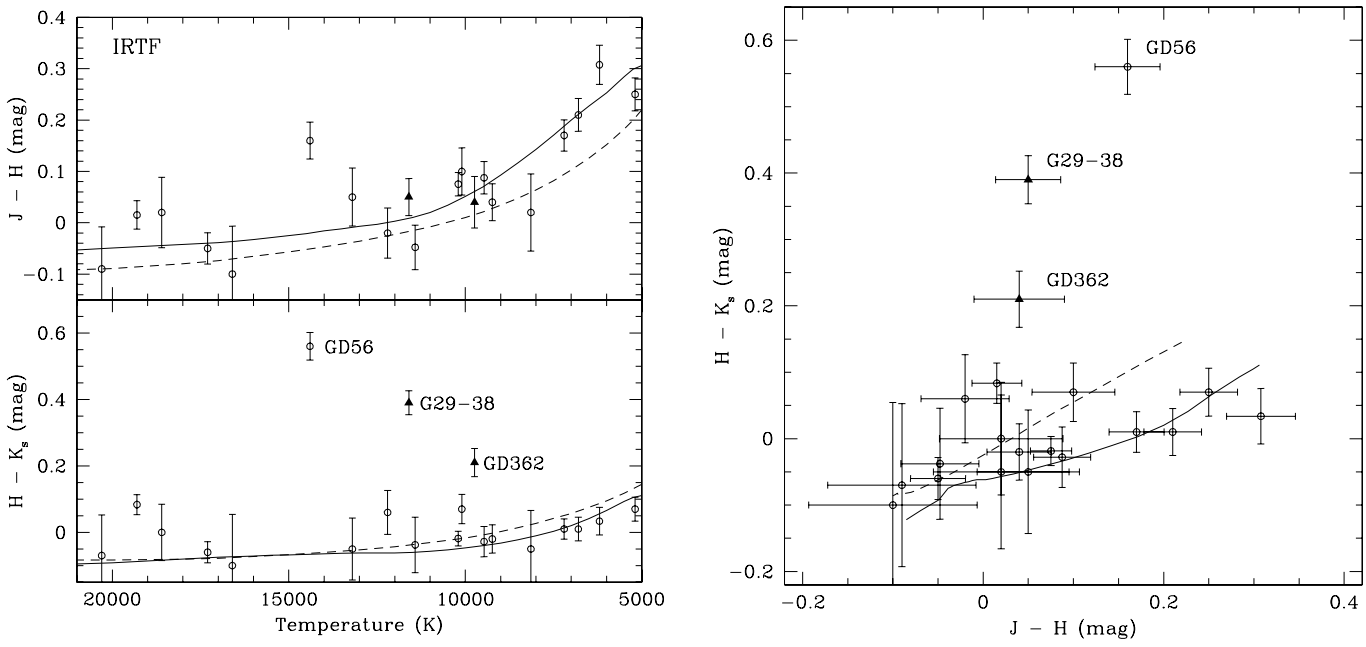


FIG. 3.—$J-H$ and $H-K$ color vs. temperature and $J-H$ vs. $H-K$ color-color diagrams for the observed DAZ stars. The predicted sequences for DA (*solid line*) and DB (*dashed line*) white dwarfs are also shown. The previously known white dwarfs with circumstellar debris disks (G29-38 and GD 362) and the newly discovered white dwarf with significant infrared excess (GD 56) are labeled.

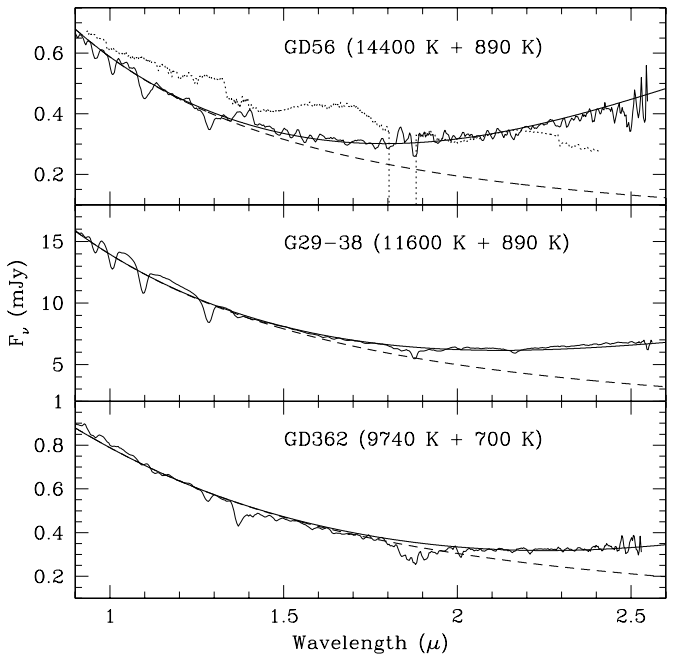


FIG. 4.—IRTF spectra of the white dwarfs with circumstellar debris disks (*jagged solid lines*). The expected near-infrared fluxes from each star (*dashed line*) and composite white dwarf and dust templates (*smooth solid line*, both blackbodies) are shown in each panel. The top panel also shows a composite blackbody + L3 dwarf template for GD 56 (*dotted line*). [*See the electronic edition of the Journal for a color version of this figure.*]

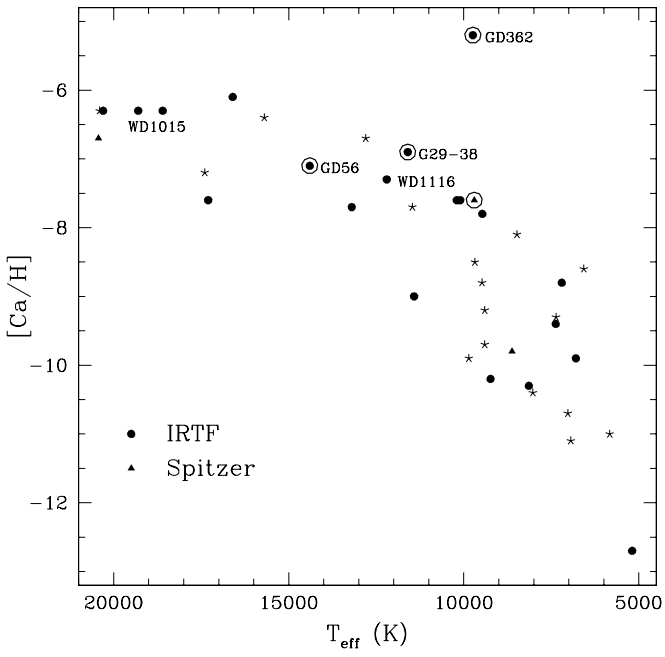


FIG. 5.—Calcium abundances vs. effective temperatures for the objects observed at the IRTF (*filled circles*) and *Spitzer* IRAC (*filled triangles*; from Reach et al. 2005; T. von Hippel et al. 2006, in preparation). The rest of the DAZs from Berger et al. (2005) are shown with star symbols. White dwarfs with circumstellar debris disks are marked with open circles. [*See the electronic edition of the Journal for a color version of this figure.*]

dwarf to a 14,400 K blackbody creates spectral features from 1.3 to 2.5 μm that are prominent, yet not seen in the spectrum of GD 56, and hence a cool dwarf companion cannot explain the excess seen between 1.5–2.5 μm. Kilic et al. (2005) could fit the observed *K*-band excess around GD 362 with a 700 K blackbody. Likewise, Reach et al. (2005) found a best-fit blackbody temperature of 890 K for the debris disk around G29-38. The top panel in Figure 4 shows that the excess around GD 56 can be explained with an ~890 K blackbody as well. Therefore, the best explanation for the *H*- and *K*-band excess in GD 56 is a circumstellar dust disk heated by the white dwarf.

GD 56 was included in the search by Farihi et al. (2005) for substellar companions around white dwarfs. They obtained *K*-band photometry for ~1/3 of their sample and used 2MASS photometry for the rest of the objects. Due to low signal-to-noise 2MASS *K*-band photometry, they did not report a near-infrared excess around GD 56 (J. Farihi 2006, private communication). Their search for excess around 371 white dwarfs resulted in the discovery of late-type stars and a brown dwarf, but no debris disks. Our IRTF search for near-infrared excess around cool DAZs has revealed two new debris disks. Our sample was restricted to 20 stars (50% of all known single DAZs) due to the positional constraints imposed by the time of the observations and the declination limit of the telescope. We observed all known DAZs with $0^h < \alpha < 11^h$ and $19^h < \alpha < 24^h$, $\delta > -17^\circ$.

A *Spitzer* IRAC search for mid-infrared excess around 4 DAZs by T. von Hippel et al. (2006, in preparation), 4 more DAZs by Debes et al. (2006, private communication), and an additional 17 DAZs by J. Farihi et al. (2006, private communication) resulted in the discovery of 2 more debris disks around cool DAZs ($T_{\rm eff} <$ 10,000 K), increasing the number of debris disks around DAZ white dwarfs to 5. There is some overlap between our IRTF program and the *Spitzer* programs; the total number of DAZs observed so far in near- or mid-infrared is 35. We estimate that the fraction of cool DAZs with detectable debris disks is 14% (5 out of 35 stars). Only 3 of the debris disks are warm enough to be detected in the *K* band, and hence the fraction of *K*-band detectable debris disks is ~9%. These discoveries suggest a growing connection between cool DAZ white dwarfs and circumstellar debris disks.

4.1. *Possible Trends*

Figure 5 shows the calcium abundances in cool DAZ white dwarfs as a function of effective temperature from Berger et al. (2005). Objects with IRTF near-infrared spectroscopy (*filled circles*), and *Spitzer* 4.5 and 8 μm photometry (*filled triangles*; T. von Hippel et al. 2006, in preparation) are also shown. The rest of the objects from the Berger et al. (2005) sample are shown as stars. Objects with circumstellar debris disks are marked with open circles.

None of the six objects with $T_{\rm eff} > 16{,}000$ K that were observed at the IRTF and with *Spitzer* IRAC show any excess emission from warm debris disks. Even though we cannot rule out the existence of cool debris disks around these objects, their high metal abundances require continuous, fairly high accretion rates from surrounding media (Koester et al. 2005; Koester & Wilken 2006). The diffusion timescales in a typical DAZ with 0.6 $M_\odot$ and $T_{\rm eff} \geq 15{,}000$ K are shorter than ~3 days (Paquette et al. 1986). Photospheric metals in these stars have to be replenished on a daily basis. If the metals were accreted from circumstellar debris disks, we should have been able to detect such disks around these objects unless all six of them have optically thin, smaller, or edge-on disks. Five of these warm DAZs are in fact more metal-rich than GD 56 and G29-38. Radiative levitation can explain the observed metal abundances in hotter white dwarfs, although it is predicted to be insignificant below 20,000 K.

All three white dwarfs with $T_{\rm eff} \sim 10{,}000$–$15{,}000$ K and $[{\rm Ca/H}] \geq -7.1$ have detectable debris disks around them. In addition, WD 1116+026 ($T_{\rm eff} = 12{,}200$ K and $[{\rm Ca/H}] = -7.3$) has

a slight (questionable) *K*-band excess that can be explained by a cooler or more distant debris disk. Its calcium abundance is 2.5 times lower than that of G29-38; therefore, unlike the warm DAZ stars mentioned above, a cooler/distant debris disk can actually explain the lower metal abundance of WD 1116+026. There is only one more white dwarf satisfying the above $T_{\rm eff}$ and [Ca/H] criteria in the Berger et al. (2005) sample. WD 1150−153 ($T_{\rm eff} = 12,800$ K and $[{\rm Ca/H}] = -6.7$) has more calcium than GD 56 and G29-38, and therefore it is likely to have a debris disk around it. HE 0106−3253 ($T_{\rm eff} = 15,700$ K and $[{\rm Ca/H}] = -6.4$) has surface temperature and calcium abundance similar to warm DAZ white dwarfs without detectable debris disks. Spectroscopic or photometric observations of both of these objects are required to search for excess flux in the infrared.

We did not detect any near-infrared excesses from debris disks in our *K*-band observations of DAZs with $T_{\rm eff} < 14,000$ K and $[{\rm Ca/H}] < -7.5$. Using *Spitzer* IRAC observations, T. von Hippel et al. (2006, in preparation) found excess 4.5 and 8 μm emission around a white dwarf with $T_{\rm eff} = 9700$ K and $[{\rm Ca/H}] = -7.6$. This object is included in Figure 1 and has $J - H = 0.11 \pm 0.06$ mag and $H - K = -0.03 \pm 0.08$ mag as measured by 2MASS. Its 2MASS colors are consistent with the predicted colors for a 9700 K white dwarf. T. von Hippel et al. (2006, in preparation) also observed a cooler DAZ white dwarf with $T_{\rm eff} = 8619$ K and a calcium abundance 2 orders of magnitude smaller, and did not find any excess up to 8 μm. The lack of infrared excess around this latter object does not mean that it does not have a debris disk, as it may have a colder, more distant debris disk, which would explain the lower calcium abundance and would show up at longer wavelengths. Four out of 10 DAZs with $T_{\rm eff} = 9000$–$15,000$ K and $[{\rm Ca/H}] > -8$ have debris disks detectable with the current precision of our observations.

5. CONCLUSIONS

Our near-infrared spectroscopic observations of 20 cool DAZs resulted in the discovery of one more white dwarf with a circumstellar debris disk. The observed *H*- and *K*-band excess around GD 56 is similar to the infrared excess seen around the previously known DAZs with circumstellar debris disks (G29-38 and GD 362). Due to its $T_{\rm eff}$ and calcium abundance (i.e., its position in Fig. 5), we postulate that another DAZ white dwarf, WD 1150−153, is likely to have a *K*-band detectable circumstellar debris disk.

The short lifetime of the hot dust (700–900 K) observed around several DAZ white dwarfs may suggest that the hot dust comes from populations of colder, longer-lived reservoirs of comets or other debris that are more massive than the hot dust clouds. Debris disks around main-sequence stars often have excesses at 24 μm, but hardly ever at 8 μm (e.g., Chen et al. 2005). DAZ white dwarfs may well behave the same way. The cool reservoir model (a cloud of dust at $\sim$120 K) may be an example of the kind of dust cloud that the recent IRAC surveys could not detect around cool DAZs, but a sensitive longer wavelength survey could. The fraction of known single DAZs with near- or mid-infrared (up to 8 μm) excesses is 14%. Mid-infrared photometry of more DAZs at longer wavelengths will likely increase this fraction. Accretion from these debris disks would also explain the photospheric metal abundances observed in DAZ white dwarfs.

Our understanding of debris disks around white dwarfs will benefit greatly from mid-infrared spectroscopy. *Spitzer* spectroscopy of G29-38 revealed a silicate feature around this object, suggesting a cometary or asteroidal origin for the debris disk (Reach et al. 2005). Mid-infrared spectroscopy of GD 56, along with the other debris disk white dwarfs, will be needed to check whether all of them show silicate emission at 10 μm. These observations will help our understanding of the formation and evolution of debris disks around white dwarfs.

We would like to thank our referee, Jay Farihi, for helpful suggestions that greatly improved the article. This material is based on work supported by the National Science Foundation under grant AST 03-07315 and the NASA grant NAG5-13094. This publication makes use of data products from the Two Micron All Sky Survey, which is a joint project of the University of Massachusetts and the Infrared Processing and Analysis Center/California Institute of Technology, funded by the National Aeronautics and Space Administration and the National Science Foundation.

REFERENCES

Alcock, C., Fristrom, C. C., & Siegelman, R. 1986, ApJ, 302, 462
Becklin, E. E., et al. 2005, ApJ, 632, L119
Berger, L., et al. 2005, A&A, 444, 565
Bergeron, P., Leggett, S. K., & Ruiz, M. T. 2001, ApJS, 133, 413
Bergeron, P., Wesemael, F., & Beauchamp, A. 1995, PASP, 107, 1047
Burleigh, M. R., Clarke, F. J., & Hodgkin, S. T. 2002, MNRAS, 331, 41
Chary, R., Zuckerman, B., & Becklin, E. E. 1999, in The Universe as Seen by ISO, ed. P. Cox & M. F. Kessler (ESA SP-427; Garching: ESA), 289
Chen, C. H., et al. 2005, ApJ, 634, 1372
Cushing, M. C., Rayner, J. T., & Vacca, W. D. 2005, ApJ, 623, 1115
Cushing, M. C., Vacca, W. D., & Rayner, J. T. 2004, PASP, 116, 362
Debes, J. H., & Sigurdsson, S. 2002, ApJ, 572, 556
Dupuis, J., Fontaine, G., Pelletier, C., & Wesemael, F. 1992, ApJS, 82, 505
Farihi, J., Becklin, E. E., & Zuckerman, B. 2005, ApJS, 161, 394
Gianninas, A., Dufour, P., & Bergeron, P. 2004, ApJ, 617, L57
Graham, J. R., Matthews, K., Neugebauer, G., & Soifer, B. T. 1990, ApJ, 357, 216
Greenstein, J. L., & Liebert, J. W. 1990, ApJ, 360, 662
Jura, M. 2003, ApJ, 584, L91
Kawka, A., & Vennes, S. 2005, in ASP Conf. Ser. 334, 14th European Workshop on White Dwarfs, ed. D. Koester & S. Moehler (San Francisco: ASP), 101
———. 2006, ApJ, 643, 402
Kepler, S. O., et al. 2005, ApJ, 634, 1311
Kilic, M., von Hippel, T., Leggett, S. K., & Winget, D. E. 2005, ApJ, 632, L115
Koester, D., & Wilken, D. 2006, A&A, in press (astro-ph/0603185)
Koester, D., et al. 2005, A&A, 432, 1025
Leggett, S. K., et al. 2002, ApJ, 564, 452
Paquette, C., Pelletier, C., Fontaine, G., & Michaud, G. 1986, ApJS, 61, 197
Rayner, J. T., et al. 2003, PASP, 115, 362
Reach, W. T., et al. 2005, ApJ, 635, L161
Vacca, W. D., Cushing, M. C., & Rayner, J. T. 2003, PASP, 115, 389
Winget, D. E. et al. 2003, in ASP Conf. Ser. 294, Scientific Frontiers in Research on Extrasolar Planets, ed. D. Deming, & S. Seager (San Francisco: ASP), 59
Zuckerman, B., & Becklin, E. E. 1987, Nature, 330, 138
Zuckerman, B., Koester, D., Reid, I. N., & Hunsch, M. 2003, ApJ, 596, 477